



Short communication

Synthesis and characterization of Pd-poly(N-vinyl-2-pyrrolidone)/KIT-5 nanocomposite for Heck reaction

Roozbeh Javad Kalbasi*, Neda Mosaddegh

Department of Chemistry, Shahreza Branch, Islamic Azad University, 311-86145 Shahreza, Isfahan, Iran

ARTICLE INFO

Article history:

Received 26 May 2011

Received in revised form 21 August 2011

Accepted 22 September 2011

Available online 29 September 2011

Keywords:

A. Composites

A. Nanostructures

B. Chemical synthesis

D. Catalytic properties

ABSTRACT

Pd-poly(N-vinyl-2-pyrrolidone)/KIT-5 nanocomposite was prepared and characterized by XRD, FT-IR, UV-vis, BET and TEM techniques. The catalytic performance of this novel heterogeneous catalyst was determined for Heck reaction. Its stability was excellent and it could be reused eight times without much loss of activity in Heck reaction.

© 2011 Elsevier Ltd. All rights reserved.

1. Introduction

Palladium-catalyzed Heck reaction between aryl halides and alkenes is one of the most valuable methods for carbon–carbon bond formation in organic synthesis [1]. Most Heck coupling reactions have been carried out in the presence of homogeneous palladium catalysts [2,3]. However, the separation and recovery of such homogeneous catalysts are not easy, and the resulting products are often contaminated by Pd. Such problems can be overcome by applying reusable and recoverable heterogeneous catalysts [4].

In catalytic applications, a uniform dispersion of nanoparticles and an effective control of particle size are usually expected. However, nanoparticles frequently aggregate to yield bulk-like materials, which greatly reduce the catalytic activity and selectivity. Therefore, they must be embedded in a matrix such as polymer [5], or immobilized in the pores of heterogeneous supports [6] like ordered mesoporous silica. However, nanoparticle-polymer composites usually suffer from disadvantages such as absence of complete heterogeneity [1]. On the other hand, although nanoparticle-mesoporous materials are completely heterogeneous, the hydrophilicity of these catalysts causes a reduction in the activity of such catalysts in organic reactions. Therefore, preparation of polymer–inorganic hybrid catalysts based on mesoporous silica materials with a hydrophobe–hydrophile nature is interesting [7–12].

Among the mesoporous materials, those consisting of interconnected large-pore cage-type mesoporous systems with three-dimensional (3D) porous networks are highly interesting, and promise supports for heterogeneous catalysis. In addition, they are considered to be more advantageous than porous materials that had a hexagonal pore structure with a two-dimensional (2D) array of pores because they allow for a faster diffusion of reactants, avoid pore blockage, provide more adsorption sites, and can be used for processing large-sized molecules. SBA-16, SBA-1, and KIT-5 are a few examples of porous materials possessing three-dimensional cage-type porous structures [13–15]. Among them, KIT-5, discovered by Ryoo et al., is a highly well-ordered cage type mesopore with cubic $Fm\bar{3}m$ closely packed symmetry, high surface area, large pores, and high specific pore volume [16]. Recently, Ryoo et al. have reported the preparation of mesoporous silica KIT-5 materials using tetraethyl orthosilicate (TEOS) as a silica source and Pluronic F127 as a structure-directing agent in an aqueous solution at low HCl concentration regime, without addition of any salt or organic additives [17]. Furthermore, it was demonstrated that a simple application of hydrothermal treatments at various temperatures ranging from 45 °C to 150 °C facilitates the tailoring of the primary mesopores, cages, and the apertures. These excellent tunable parameters and interesting structure of KIT-5 potentially allow one to use them as inorganic support for making heterogeneous catalysts.

In continuing the previous activities to develop new organic–inorganic hybrid materials as heterogeneous catalysts [9–12], herein, a heterogeneous catalyst is introduced using a cage-type mesoporous system with 3D porous networks. The catalytic activity of this nanocomposite (Pd-poly(N-vinyl-2-pyrrolidone)/KIT-5) was

* Corresponding author. Tel.: +98 321 3213211; fax: +98 321 3213103.
E-mail addresses: rkalbasi@iaush.ac.ir, rkalbasi@gmail.com (R.J. Kalbasi).

tested for Heck reaction. This catalyst could be reused several times (at least 8) without significant loss of activity/selectivity.

2. Experimental method

2.1. Catalyst characterization

The samples were analyzed using FT-IR spectroscopy (using a Perkin Elmer 65 in KBr matrix in the range of 4000–400 cm^{-1}). The BET specific surface areas and BJH pore size distribution of the samples were determined by adsorption–desorption of nitrogen at liquid nitrogen temperature, using a Series BEL SORP 18. The X-ray powder diffraction (XRD) of the catalyst was carried out on a Bruker D8Advance X-ray diffractometer using nickel filtered Cu K α radiation at 40 kV and 20 mA. Moreover, X-ray photoelectron spectra (XPS) was recorded on ESCA SSX-100 (Shimadzu) using a non-monochromatized Mg K α X-ray as the excitation source. The thermal gravimetric analysis (TGA) data were obtained by a Setaram Labsys TG (STA) in a temperature range of 30–650 °C and heating rate of 10 °C/min in N $_2$ atmosphere. Transmission electron microscope (TEM) observations were performed on a JEOL JEM.2011 electron microscope at an accelerating voltage of 200.00 kV using EX24093JGT detector in order to obtain information on the size of Pd nanoparticles and the DRS UV–vis spectra were recorded with JASCO spectrometer, V-670 from 190 to 2700 nm.

2.2. Catalyst preparation

The cage-type mesoporous silica KIT-5 was prepared through the method described in the literature recently [15].

Pd-poly(N-vinyl-2-pyrrolidone)/KIT-5 was synthesized in two steps. At first, poly(N-vinyl-2-pyrrolidone)/KIT-5 (PVP/KIT-5) was prepared. N-vinyl-2-pyrrolidone (NVP) (0.5 mL, 4.6 mmol) and KIT-5 (0.5 g) in 7 mL tetrahydrofuran (THF) were placed in a round bottom flask. Benzoyl peroxide (0.034 g) was added and the mixture was heated to 65–70 °C for 5 h while being stirred under N $_2$ gas. The resulting white fine powder composite (PVP/KIT-5) was collected by filtration, washed several times with THF, and finally dried at 60 °C under reduced pressure.

In the second step, PVP/KIT-5 (0.5 g) and 10 mL of an aqueous acidic solution ($C_{\text{HCl}} = 0.09 \text{ M}$) of Pd(OAc) $_2$ (0.053 g, 0.236 mmol) were placed in a round bottom flask. The mixture was heated to 80 °C for 5 h while being stirred under N $_2$ gas. Then, 0.6 mL (9.89 mmol) aqueous solution of hydrazine hydrates (N $_2$ H $_4$ ·H $_2$ O) (80 vol.%) was added to the mixture drop by drop in 15–20 min. After that, the solution was stirred at 60 °C for 1 h. Afterwards, it was filtered and washed sequentially with chloroform and methanol to remove excess N $_2$ H $_4$ ·H $_2$ O, and was dried in room temperature to yield Pd-poly(N-vinyl-2-pyrrolidone)/KIT-5 (Pd-PVP/KIT-5) nanocomposite. The Pd content of the catalyst estimated by ICP-AES was 0.374 mmol g $^{-1}$.

2.3. General procedure for Heck reaction

In the typical procedure for Heck coupling reaction, a mixture of iodobenzene (1 mmol), styrene (2 mmol), K $_2$ CO $_3$ (5 mmol), and catalyst (0.14 g, Pd-PVP/KIT-5) in MeOH/H $_2$ O (3/1, v/v) (5 mL) was placed in a round bottom flask. The suspension was stirred at 60 °C for 2 h. The progress of reaction was monitored by TLC using n-hexane as eluent. After completion of the reaction (monitored by TLC), for the reaction work-up, the catalyst was removed from the reaction mixture by filtration, and then the reaction product was extracted with CH $_2$ Cl $_2$ (3 \times 5 mL). The solvent was removed under reduced pressure. The crude product was purified by flash column chromatography to afford the desired coupling product (96%

isolated yield). The product was identified with ^1H NMR, ^{13}C NMR and FT-IR spectroscopy techniques.

3. Results and discussion

3.1. Catalyst characterization

Fig. 1 shows the powder XRD patterns of the silica KIT-5, PVP/KIT-5 and Pd-PVP/KIT-5. Purely siliceous KIT-5 exhibits three reflections in the region $2\theta = 0.7\text{--}3^\circ$ which can be indexed to the (1 1 1), (2 0 0), and (2 2 0) reflections of cubic space group *Fm*3*m* [15]. The PVP/KIT-5 and Pd-PVP/KIT-5 ($2\theta = 0.7\text{--}10^\circ$) samples show the same pattern indicating that the structure of the KIT-5 (1 0 0) is well retained even after immobilization (Fig. 1). However, the intensity of the characteristic reflection peaks of the PVP/KIT-5 and Pd-PVP/KIT-5 samples are found to be reduced (Fig. 1). This may be attributed to the symmetry destroyed by the hybridization of KIT-5 which is also found in the ordered mesoporous silica loading with guest matter [18].

The length of the cubic cell a_0 is calculated by using the formula $a_0 = d_{111}\sqrt{3}$ (Table 1). Compared to the d -spacing (or the pore center distance a_0) of KIT-5 and PVP/KIT-5, the incorporation of the Pd nanoparticles into PVP/KIT-5 pores leads to the expansion of the KIT-5 pore array (Table 1). These results are in good agreement with that obtained in BET observations.

The wide-angle XRD pattern of the Pd-PVP/KIT-5 nanocomposite ($2\theta = 30\text{--}90^\circ$) (Fig. 1) shows the reflections at 39.92°, 46.54°, 67.90° and 81.84°; and these peaks correspond to (1 1 1), (2 0 0), (2 2 0) and (3 1 1) lattice planes of Pd nanoparticles [19]. Planes were assigned by being compared with Pd standard, and they correspond to the *fcc* crystal lattice structure of Pd (JCPDS, Card No.

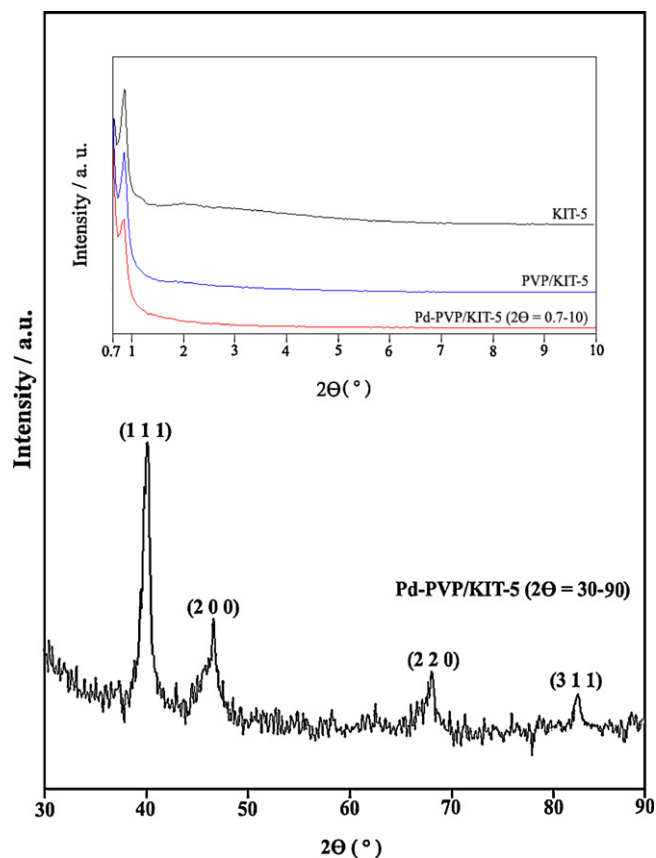


Fig. 1. The powder XRD pattern of (a) mesoporous silica KIT-5, (b) PVP/KIT-5 and (c) Pd-PVP/KIT-5.

Table 1Physicochemical properties of mesoporous silica KIT-5, PVP/KIT-5 and Pd-PVP/KIT-5 samples obtained from XRD and N₂ adsorption.

Sample	BET surface area (m ² g ⁻¹)	V _p (cm ³ g ⁻¹) ^a	BJH pore diameter (nm)	d ₁₁₁ (nm)	a ₀ (nm) ^b
Mesoporous silica KIT-5	1090	0.71	2.62	10.38	17.98
PVP/KIT-5	611	0.41	2.68	10.51	18.20
Pd-PVP/KIT-5	305	0.40	5.48	11.13	19.27

^a Total pore volume.^b Unit cell parameter.

05-0681). The crystallite size of Pd particles was evaluated using Scherrer equation which was found to be approx. 7 nm in size. The size of the Pd nanoparticles, determined by using TEM analysis, is more reliable than that determined by using Scherrer formula in XRD analysis.

Fig. 2 presents the FT-IR spectra of KIT-5 (a), PVP/KIT-5 (b), and Pd-PVP/KIT-5 (c). Similar to mesoporous silica KIT-5 (Fig. 2a), PVP/KIT-5 and Pd-PVP/KIT-5 samples show the typical vibrations of asymmetric and symmetric stretching as well as the rocking of Si–O–Si at around 1080, 816, and 458 cm⁻¹ (Fig. 2). The existence of PVP in the PVP/KIT-5 composite is evidenced by the appearance of typical PVP vibration on the FT-IR spectrum (Fig. 2b). In the FT-IR spectrum of PVP/KIT-5 (Fig. 2b), the new band at 1663 cm⁻¹ corresponds to the carbonyl bond of PVP [20]. Moreover, the presence of peaks at around 2800–3000 cm⁻¹ corresponds to the aliphatic C–H stretching in PVP/KIT-5 (Fig. 2b). As shown in Pd-PVP/KIT-5 spectrum (Fig. 2c), the band around 1663 cm⁻¹,

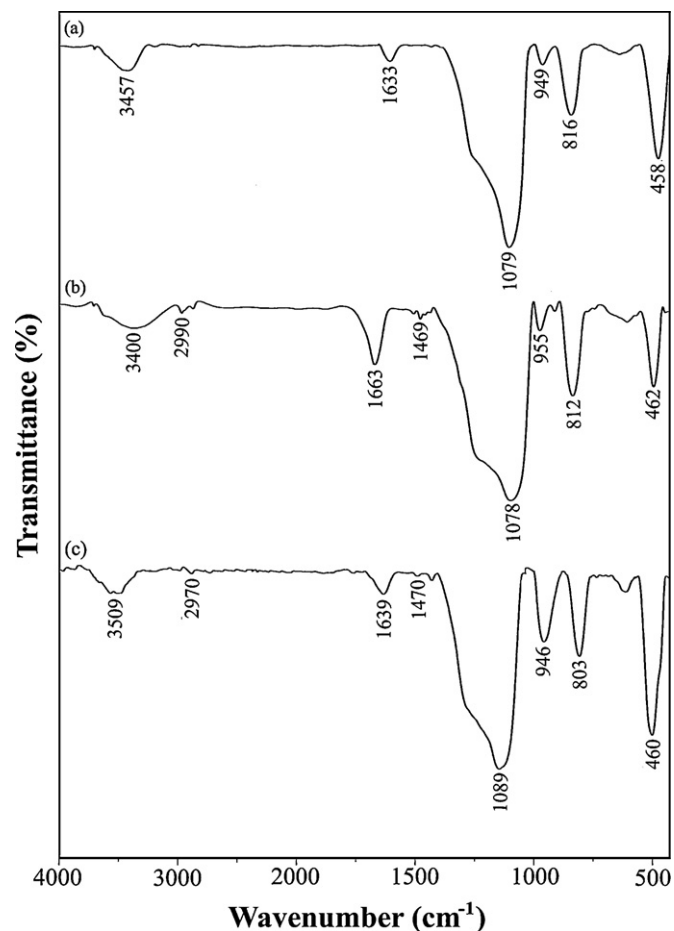


Fig. 2. FT-IR spectra of (a) mesoporous silica KIT-5, (b) PVP/KIT-5 and (c) Pd-PVP/KIT-5.

corresponding to carbonyl bond of PVP, is shifted to lower wave numbers (1639 cm⁻¹). Moreover, the peak intensity of the carbonyl bond in the spectrum of Pd-PVP/KIT-5 is lower than that of PVP/KIT-5. This may be due to the interaction between Pd nanoparticles and C=O groups. This means that the double bond CO stretches become weak by being coordinated with Pd nanoparticles [20].

Fig. 3 presents the TGA curves of KIT-5 (a), PVP (b), PVP/KIT-5 (c) and Pd-PVP/KIT-5 (d) under N₂ atmosphere. The mass loss at temperature <100 °C (around 3.5%, w/w) is attributed to desorption of water present in the surfaces of the KIT-5 (Fig. 3a). The TGA curve of PVP shows a small mass loss (around 7.5%, w/w) in the temperature range of 50–150 °C, which is apparently associated with adsorbed water (Fig. 3b). At temperatures above 200 °C, PVP shows one main stage of degradation. The mass loss for PVP in the second step is equal to 77% (w/w) which corresponds to the effective degradation of the polymer (Fig. 3b). Thermo analysis of PVP/KIT-5 shows two steps of mass loss (Fig. 3c). The first step (around 3%, w/w) that occurs at 70 °C is related to desorption of water. The second step (around 9%, w/w) which appeared at 270 °C is attributed to degradation of the polymer, which ended at 580 °C (Fig. 3c). By comparing the PVP and PVP/KIT-5 curves, one can find that the weight loss of PVP/KIT-5 occurs at a higher temperature, it illustrates that PVP/KIT-5 has higher thermal stability and slower degradation rate than PVP (Fig. 3b and c). However, for Pd-PVP/KIT-5 sample, two separate weight loss steps are seen (Fig. 3d). The first step (around 3%, w/w) appearing at temperature <100 °C corresponds to the loss of water. The second weight loss (about 500–580 °C) of around 8% (w/w) is related to the degradation of the polymer. Obviously, the hybrid Pd-PVP/KIT-5 shows slower degradation rate than PVP/KIT-5, which may be attributed to the presence of Pd nanoparticles in the composite structure. By comparing the TGA curves of

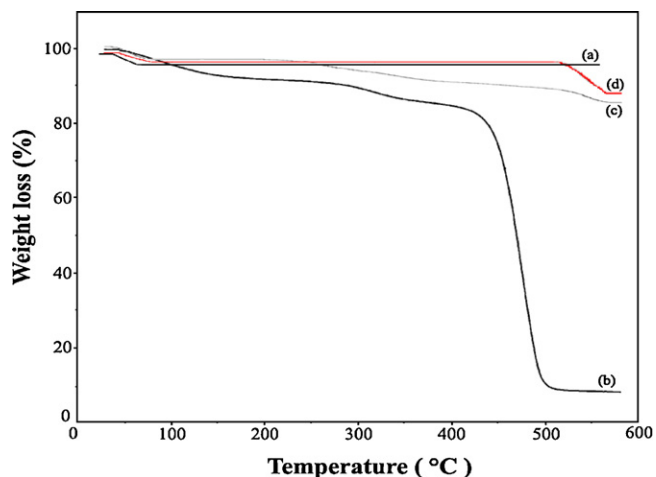


Fig. 3. TGA curves of (a) mesoporous silica KIT-5, (b) PVP, (c) PVP/KIT-5 and (d) Pd-PVP/KIT-5.

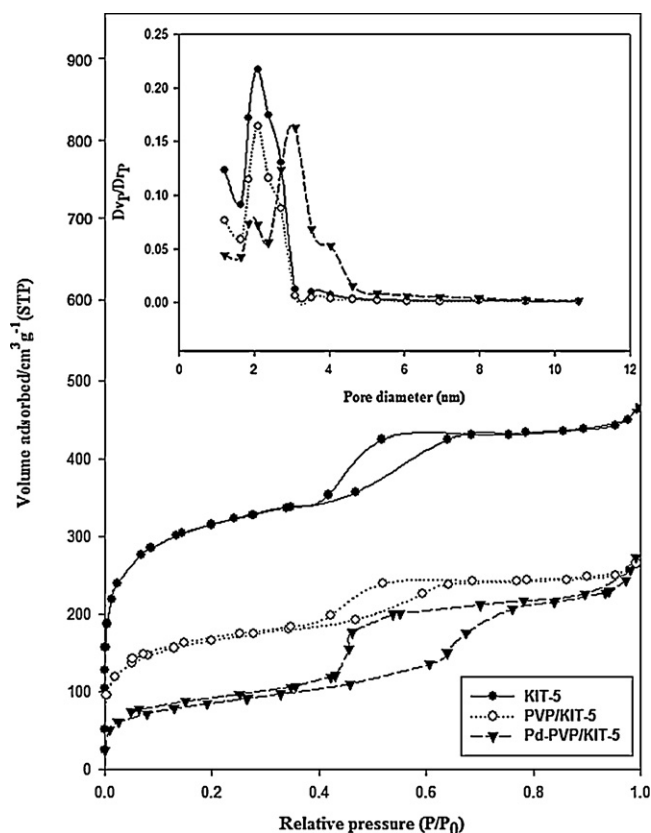


Fig. 4. N_2 adsorption-desorption isotherms of mesoporous silica KIT-5, PVP/KIT-5 and Pd-PVP/KIT-5. Inset: pore size distribution.

PVP/KIT-5 (Fig. 3c) and Pd-PVP/KIT-5 (Fig. 3d), it can be found that polymer content of composite was not significantly changed after the Pd loading. Therefore, the assumption that palladium nanoparticles interact with the polymer carbonyl groups (present in the FT-IR section) can be proved. Because the amounts of polymer in composites are approximately equal, it can be found that the weakness of carbonyl bond vibration is due to the interaction between Pd nanoparticles and the polymer and that the decrease in the intensity of carbonyl bond after Pd loading is not related to the decrease in the polymer contents of the composite.

The BET specific surface areas and the pore sizes of KIT-5, PVP/KIT-5 and Pd-PVP/KIT-5 were calculated using BET and BJH methods (Table 1). All the samples exhibit a type IV adsorption isotherm with an H_2 hysteresis loop, typically observed for the mesoporous samples with a cage-type pore structure (Fig. 4). The

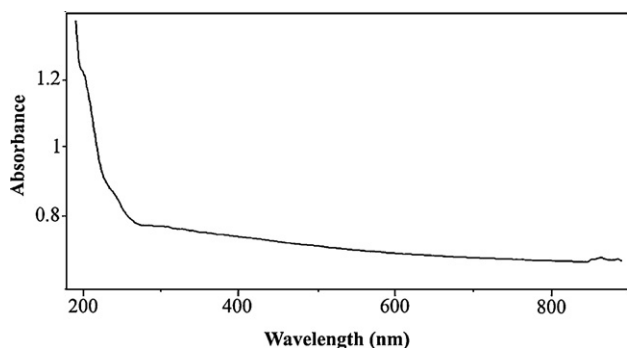


Fig. 5. UV-vis spectra of Pd-PVP/KIT-5.

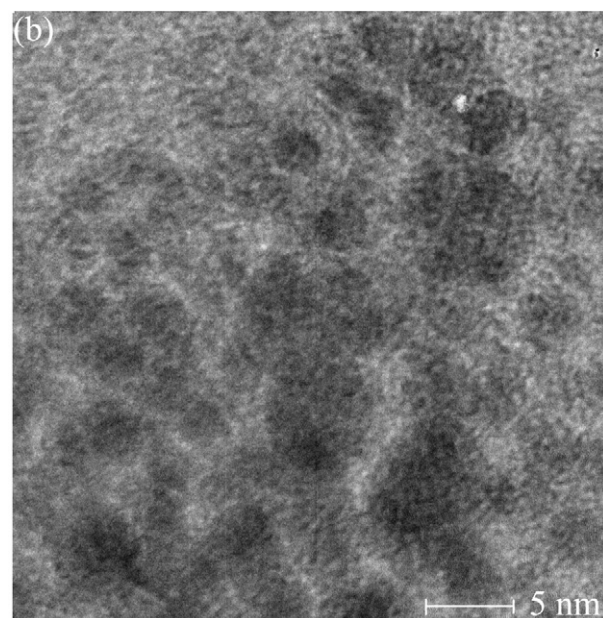
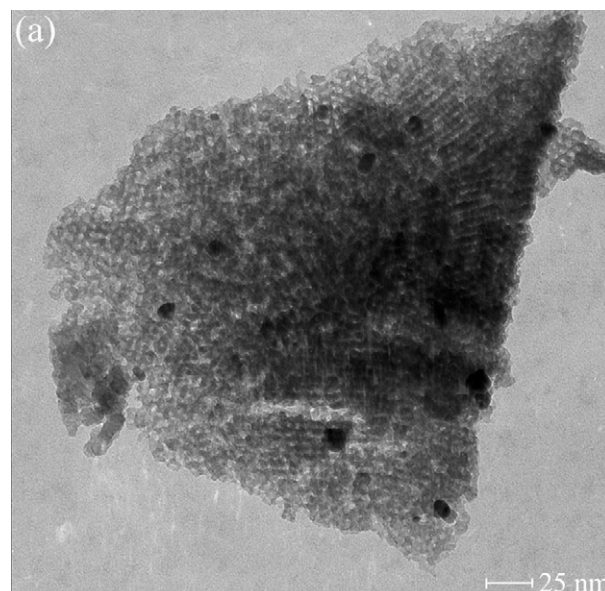


Fig. 6. TEM images for Pd-PVP/KIT-5.

corresponding BJH pore size distribution curves for the KIT-5, PVP/KIT-5 and Pd-PVP/KIT-5 materials are shown in Fig. 4. It is clear that PVP/KIT-5 and Pd-PVP/KIT-5 exhibit a smaller specific surface area in comparison to those of pure KIT-5 (Table 1). However, there is a noticeable increase in pore diameter for Pd-PVP/KIT-5 which may be due to the incorporation of Pd nanoparticles into PVP/KIT-5. Similar results were reported for Pt encapsulated in SBA-15 [21].

Fig. 5 displays the result of UV-vis spectra of Pd-PVP/KIT-5. The UV-vis spectra of $Pd(OAc)_2$ which reveal a peak at 400 nm refer to the existence of Pd(II) [22]. As mentioned in the experimental section, Pd(0)-PVP/KIT-5 was prepared by adding hydrazine hydrate to Pd(II)-PVP/KIT-5. However, as can be seen in Fig. 5, there is not any peak at 400 nm in the UV-vis spectra of Pd-PVP/KIT-5, which indicates complete reduction of Pd(II) to Pd nanoparticles.

The TEM micrographs of Pd-PVP/KIT-5 showed that the ordered cubic $Fm\bar{3}m$ mesostructure of KIT-5 was retained, and no damage in the periodic structure of the silicate framework was observed (Fig. 6a). The places with darker contrasts could be assigned to the

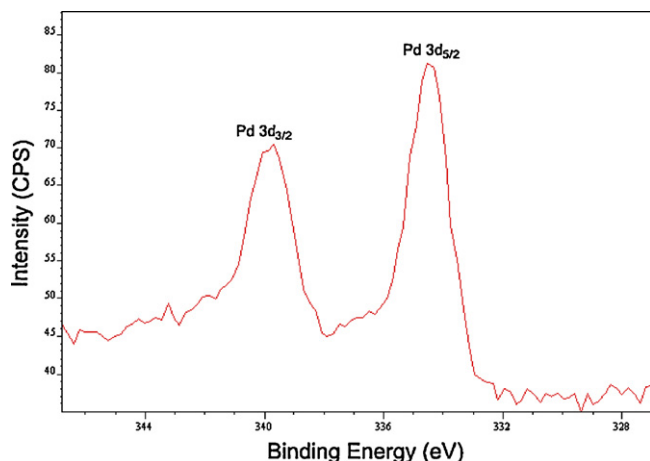


Fig. 7. XPS spectrum of Pd 3d of Pd-PVP/KIT-5.

presence of Pd particles with different dispersion. This assumption was confirmed by EDX data, in which the estimated Pd/Si ratio was about 0.04 and it correlated with the loaded Pd amount. The small dark spots in the images could be ascribed to Pd nanoparticles, probably located in the support channels. The larger dark areas over the channels most likely corresponded to Pd nanoparticle agglomerate on the external surface.

Fig. 6b shows that the sizes of Pd nanoparticles were around 3–5 nm, which were a little larger than the silica mesopore diameter (2.6 nm). With the incorporation of the nanoparticles larger than the structure directing agent, pore size can expand the entire mesopore structure uniformly [23]. These are in accordance with BET and XRD results.

To obtain information on the structural features of the Pd-PVP/KIT-5 catalyst, X-ray photoelectron spectroscopy (XPS) study has been carried out on the Pd-PVP/KIT-5 catalyst. The XPS result of Pd nanoparticles dispersed in PVP/KIT-5 media for Pd 3d spectrum with the binding energies of Pd 3d_{5/2} and Pd 3d_{3/2} lying at about 334.3 and 339.5 eV, respectively (see Fig. 7). It means that Pd nanoparticles are stable as metallic state in PVP/KIT-5 media (the XPS spectrum of Pd(II) ions reveals two peaks at about 337 and 342 eV refer to Pd 3d_{5/2} and 3d_{3/2} [24]). In comparison to the standard binding energy (Pd⁰ with Pd 3d_{5/2} of about 335 eV and Pd_{3/2} of about 340 eV) [25], it can be concluded that the Pd peaks in Pd-PVP/KIT-5 shifted to lower binding energy than Pd⁰ standard

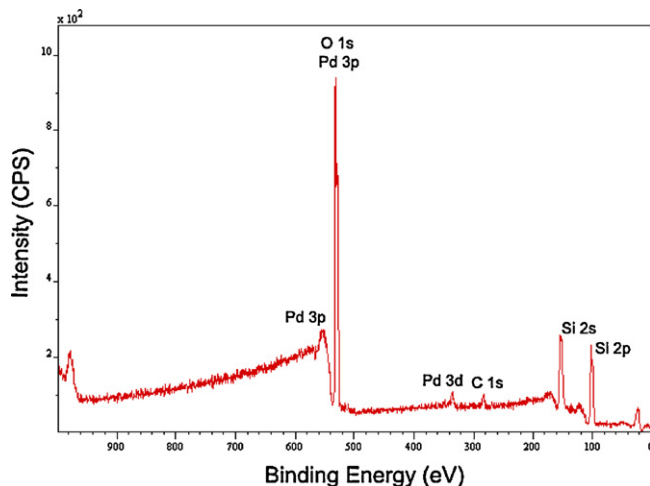


Fig. 8. Full XPS spectrum of Pd-PVP/KIT-5.

Table 2

Effect of different bases and solvents on Heck reaction.^{a,b}

Base	Yield (%) ^c	Time (h)
K ₂ CO ₃ ^d	96	2
K ₂ CO ₃ ^e	80	6
Na ₃ PO ₄ ^d	60	2
Et ₃ N ^d	25	2

^a Reaction conditions: Pd-PVP/KIT-5 (0.14 g), iodobenzene (1 mmol), styrene (2 mmol), base (5 equiv.), 60 °C.

^b (*E*)/(*Z*) stereoselectivity was higher than 99:1.

^c Isolated yield related to *E* isomer.

^d Solvent: MeOH/H₂O (3:1, v/v) (5 mL).

^e Solvent: H₂O (5 mL).

binding energy. As we know, the position of Pd 3d peak is usually influenced by the local chemical/physical environment around Pd species besides the formal oxidation state, and shifts to lower binding energy when the charge density around it increases [25]. So, the peaks at (334.3 and 339.5 eV) should be due to Pd⁰ species bound directly to O of carbonyl group or N of PVP. The contribution of the charge transfer of N and O of PVP to Pd⁰ results in the increase in the charge density around Pd⁰ and the decrease in binding energy.

The full XPS spectrum of Pd-PVP/KIT-5 showed peaks of carbon, oxygen, silicon and palladium. Silicon peaks correspond to mesoporous silica KIT-5 structure and carbon is related to the PVP structure (Fig. 8).

3.2. Catalytic activity

Pd-PVP/KIT-5 nanocomposite was used as a catalyst for Heck reactions of various aryl halides with styrene.

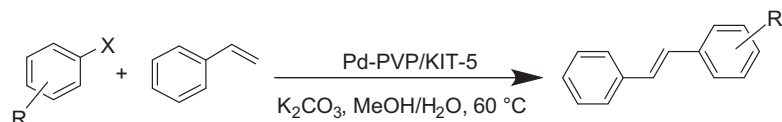
To optimize the reaction conditions, a model reaction was carried out by taking iodobenzene and styrene in different solvents and bases at 60 °C. Solvent plays a crucial role in the rate and product distribution of Heck reactions. In this context, two kinds of green solvents were used: H₂O or MeOH/H₂O (3:1, v/v); and the reaction was catalyzed with 0.14 g of Pd-PVP/KIT-5 (Table 2). The experimental results showed that the time it took for the reaction to be completed was rarely shorter in the case of using MeOH/H₂O (3:1, v/v) as a solvent and the yield was higher. Hence, MeOH/H₂O (3:1, v/v) was chosen as solvent.

The effect of base on the coupling reaction was evaluated by taking iodobenzene with styrene in MeOH/H₂O (3:1, v/v) at 60 °C in the presence of Pd-PVP/KIT-5 with various bases (K₂CO₃, Et₃N, and Na₃PO₄) (Table 2). The results revealed that the inorganic bases which were used were more effective than Et₃N; and hence, the economically cheaper K₂CO₃ was chosen as the base for the coupling reactions.

In order to discriminate the effect of Pd-PVP/KIT-5, the reaction occurred over palladium nanoparticles in the same reaction conditions, and no activity was seen in this condition.

Heck reactions of different aryl halides and styrene over Pd-PVP/KIT-5 as catalyst were investigated (Table 3) [3,26]. The turnover frequency (TOF) value indicates that the Pd-PVP/KIT-5 is a potential candidate for this kind of reaction, TOF being defined as the mol product/(mol catalyst h); and this was calculated from the isolated yield, the amount of palladium used and the reaction time.

Reusability of the catalyst was tested by carrying out repeated runs of the reaction on the same batch of the catalyst in the case of the model reaction (Table 4). The results showed that this catalyst could be reused eight times without any modification and that no significant loss of activity/selectivity performance was observed. In addition, there was very low Pd leaching during the reaction (Table 4). Compared to our previous work on composites based on SBA-15

Table 3Heck reaction of aromatic aryl halides and styrene catalyzed by Pd-PVP/KIT-5.^{a,b}

Entry	Substrate	Product	Yield (%) ^c	TOF (h ⁻¹) ^d	Time (h)	Mp (°C)	
						Found	Reported [Ref.]
1			96	9.25	2	122–124	121–123 [3]
2			97	1.56	12	136–138	135–137 [3]
3			95	3.66	5	117–119	116–118 [3]
4			96	18.5	1	38–40	38–39 [22]
5			96	2.31	8	122–124	121–123 [3]
6			63	1.01	12	142–144	142–145 [3]
7			85	1.36	12	122–124	121–123 [3]

^a Reaction conditions: Pd-PVP/KIT-5 (0.14 g), iodobenzene (1 mmol), styrene (2 mmol), K₂CO₃ (5 equiv.), MeOH/H₂O (3:1, v/v), 60 °C.^b (*E*)/(*Z*) stereoselectivity was higher than 99:1.^c Isolated yield related to *E* isomer.^d Turn-over frequency.**Table 4**The catalyst reusability for the Heck reaction.^{a,b}

Cycle	Yield (%) ^c	Pd content of catalyst (mmol)
Fresh	96	0.0519
1	96	0.0519
2	96	0.0519
3	96	0.0519
4	94	0.0519
5	94	0.0518
6	93	0.0518
7	93	0.0518
8	91	0.0517

^a Reaction conditions: Pd-PVP/KIT-5 (0.14 g), iodobenzene (1 mmol), styrene (2 mmol), K₂CO₃ (5 equiv.), MeOH/H₂O (3:1 v/v) (5 mL), 60 °C, 2 h.^b (*E*)/(*Z*) stereoselectivity was higher than 99:1.^c Isolated yield related to *E* isomer.

[9–12], Pd-PVP/KIT-5 showed more recyclability, which could be related to the interconnected large-pore cage-type mesoporous KIT-5 with 3D porous networks in comparison to SBA-15 with a 2D array of pores because three-dimensional porous network of KIT-5 allows for a faster diffusion of reactants, avoids pore blockage, provides more adsorption sites and can prevent leaching of Pd nanoparticles. The XRD patterns of the used catalyst showed that the structure of the catalyst was maintained.

Table 5 shows a comparison between the catalyst used in the present study and other Pd catalysts reported in the literature for Heck reaction [27–31]. As can be seen, Pd-PVP/KIT-5 catalyst shows good activity and reasonable yield for Heck reaction of iodobenzene and styrene in a reasonable time with high yields in the presence of a green solvent. In addition, the reusability of Pd-PVP/KIT-5 was considerable.

Table 5

Comparison of catalytic activity of Pd-PVP/KIT-5 with other catalysts.

Catalyst	Substrate	Product	Solvent	Temperature (°C)	Yield (%)	Time (h)	Ref.
Pd-TiO ₂	Iodobenzene	E-Stilbene	NMP	120	98	0.5	[27]
Pd-complex	Iodobenzene	E-Stilbene	Toluene-PEG600 (3:1)	80	98	5	[28]
Pd/NF300	Iodobenzene	E-Stilbene	DMF	80–140	97	4	[29]
Polyion complex	Iodobenzene	E-Stilbene	H ₂ O	80	99	20	[30]
Pd-polymer composite	Iodobenzene	E-Stilbene	DMF	80	89	8	[31]
Pd-PVP/KIT-5	Iodobenzene	E-Stilbene	MeOH/H ₂ O (3:1, v/v)	60	96	2	This work

4. Conclusion

A novel polymer–inorganic hybrid material, Pd nanoparticle-PVP/KIT-5, was prepared by a simple method. The catalytic activity of this novel catalyst was excellent for Heck reaction of aryl chloride, bromide and iodides under aerobic conditions. This heterogeneous catalyst can practically replace a homogeneous catalyst in view of the following advantages: (a) high catalytic activity under mild reaction conditions and (b) reusability of the catalyst for several times without any significant loss in the yield of the reaction.

Acknowledgements

The support by the Islamic Azad University, Shahreza Branch (IAUSH) Research Council and Center of Excellence in Chemistry is gratefully acknowledged.

References

- [1] A.M. Trzeciak, J.J. Ziółkowski, *Coord. Chem. Rev.* 251 (2007) 1281–1293.
- [2] C.A. Fleckenstein, H. Plenio, *Chem. Soc. Rev.* 39 (2010) 694–711.
- [3] N. Iranpoor, H. Firouzabadi, A. Tarassoli, M. Fereidoonzehad, *Tetrahedron* 66 (2010) 2415–2421.
- [4] L. Yin, J. Liebscher, *Chem. Rev.* 107 (2007) 133–173.
- [5] R.U. Islam, M.J. Witcomb, M.S. Scurrill, W. Van Otterlo, K. Mallick, *Catal. Commun.* 12 (2010) 116–121.
- [6] I. Yuranov, P. Moeckli, E. Suvorova, P. Buffat, L. Kiwi-Minsker, A. Renken, *J. Mol. Catal. A: Chem.* 192 (2003) 239–251.
- [7] G. Morales, R. van Grieken, A. Martín, F. Martínez, *Chem. Eng. J.* 161 (2010) 388–396.
- [8] Z.H. Ma, H.B. Han, Z.B. Zhou, J. Nie, *J. Mol. Catal. A: Chem.* 311 (2009) 46–53.
- [9] R.J. Kalbasi, M. Kolahdoozan, A.R. Massah, K. Shahabian, *Bull. Kor. Chem. Soc.* 31 (2010) 2618–2626.
- [10] R.J. Kalbasi, M. Kolahdoozan, M. Rezaei, *Mater. Chem. Phys.* 125 (2011) 784–790.
- [11] R.J. Kalbasi, A.A. Nourbakhsh, F. Babaknezhad, *Catal. Commun.* 12 (2011) 955–960.
- [12] R.J. Kalbasi, M. Kolahdoozan, K. Shahabian, F. Zamani, *Catal. Commun.* 11 (2010) 1109–1115.
- [13] E.M. Rivera-Muñoz, R. Huirache-Acuña, *Int. J. Mol. Sci.* 11 (2010) 3069–3086.
- [14] M.-C. Liu, C.-S. Chang, J.C.C. Chan, H.-S. Sheu, S. Cheng, *Micropor. Mesopor. Mater.* 121 (2009) 41–51.
- [15] W. Cheng-Yu, H. Ya-Ting, Y. Chia-Min, *Micropor. Mesopor. Mater.* 117 (2009) 249–256.
- [16] F. Kleitz, D. Liu, G.M. Anilkumar, I.-S. Park, L.A. Solovyov, A.N. Shmakov, R. Ryoo, *J. Phys. Chem. B* 107 (2003) 14296–14300.
- [17] F. Kleitz, T.-W. Kim, R. Ryoo, *Bull. Kor. Chem. Soc.* 26 (2005) 1653–1668.
- [18] T. Tsoncheva, L. Ivanova, J. Rosenholm, M. Linden, *Appl. Catal. B: Environ.* 89 (2009) 365–374.
- [19] P. Wang, Z. Wang, J. Li, Y. Bai, *Micropor. Mesopor. Mater.* 116 (2008) 400–405.
- [20] T. Iwamoto, K. Matsumoto, T. Matsushita, M. Inokuchi, N. Toshima, *J. Colloid Interface Sci.* 336 (2009) 879–888.
- [21] H. Song, R.M. Rioux, J.D. Hoefelmeyer, R. Komor, K. Niesz, M. Grass, P. Yang, G.A. Somorjai, *J. Am. Chem. Soc.* 128 (2006) 3027–3037.
- [22] P. Ahmadian Namini, A.A. Babaluo, B. Bayati, *Int. J. Nanosci. Nanotechnol.* 3 (2007) 37–43.
- [23] Z. Konya, V.F. Puentes, I. Kiricsi, J. Zhu, A.P. Alivisatos, G.A. Somorjai, *Nano Lett.* 2 (2002) 907–910.
- [24] A. Gniewek, A.M. Trzeciak, J.J. Ziółkowski, L. Kepinski, J. Wrzyszczyk, W. Tylus, *J. Catal.* 229 (2005) 332–343.
- [25] T. Teranishi, M. Miyake, *Chem. Mater.* 10 (1998) 594–600.
- [26] Y. Leng, F. Yang, K. Wei, Y. Wu, *Tetrahedron* 66 (2010) 1244–1248.
- [27] E.A. Obuya, W. Harrigana, D.M. Andala, J. Lippens, T.C. Keane, W.E. Jones Jr., *Tetrahedron Lett.* 340 (2011) 89–98.
- [28] D. Sawant, Y. Wagh, K. Bhatte, A. Panda, B. Bhanage, *Tetrahedron Lett.* 52 (2011) 2390–2393.
- [29] Z. Gao, Y. Feng, F. Cui, Z. Hua, J. Zhou, Y. Zhu, J. Shi, *J. Mol. Catal. A: Chem.* 336 (2011) 51–57.
- [30] A. Ohtaka, Y. Tamaki, Y. Igawa, K. Egamia, O. Shimomura, R. Nomura, *Tetrahedron* 66 (2010) 5642–5646.
- [31] R.U. Islam, M.J. Witcomb, M.S. Scurrill, W.V. Otterlo, K. Mallick, *Catal. Commun.* 12 (2010) 116–121.